A hybrid CFD RANS/Lagrangian approach to model atmospheric dispersion of pollutants in complex urban geometries

Meissam L. Bahlali*, Eric Dupont and Bertrand Carissimo

CEREA,
Joint laboratory École des Ponts ParisTech/EDF R&D,
Université Paris-Est,
Marne-la-Vallée, France
Email: meissambahlali@gmail.com
Email: eric.dupont@edf.fr
Email: bertrand.carissimo@enpc.fr
*Corresponding author

Abstract: Lagrangian atmospheric dispersion models consist of tracking the trajectories of particles of pollutant emitted into the atmosphere. In this paper, the objective is to compare the Lagrangian and Eulerian dispersion models in the same computational fluid dynamics code (*Code_Saturne*), therefore using the same wind and turbulence fields for both. The Lagrangian stochastic model used in this work is the *simplified Langevin model* (SLM) of Pope (1985, 2000) and pertains to the approaches referred to as probability density function methods. This model has been extensively used in turbulent combustion or multiphase flows, but to our knowledge, it has not been used in atmospheric dispersion applications. First, we show that the SLM respects the well-mixed criterion. Then, we validate the model in the case of a continuous point release with uniform mean wind speed and turbulent diffusivity. Finally, we validate the model with an experimental campaign involving a stably stratified surface layer.

Keywords: atmospheric dispersion; Lagrangian stochastic modelling; turbulence; computational fluid dynamics; CFD; environmental pollution.

Biographical notes: Meissam L. Bahlali is an Engineer and Master's in Fluid Mechanics and Energy Science. She is also a PhD student at CEREA on the subject of 'Adaptation of the hybrid Eulerian/Lagrangian stochastic model of the CFD code *Code_Saturne* to pollutant atmospheric dispersion at the micro-meteorological scale and comparison with the Eulerian method'.

Eric Dupont is an Expert Scientist at CEREA and EDF R&D and specialises in dynamics of the lower atmosphere. His work focuses on the modelling of atmospheric flows and pollutant dispersion at different spatial scales (from mesoscale to microscale).

Bertrand Carissimo is a Senior Scientist at CEREA and EDF R&D and specialises in atmospheric environment. His work focuses on micro-meteorological modelling as well as pollutant dispersion at very local scale around industrial sites and wind farms.

1 Introduction

A cloud of pollutants released into the atmosphere is subject to various processes, among which the two main processes involved in this paper are: advection and diffusion. By definition, the turbulent dispersion is characterised by the combination of advection and turbulent diffusion. This phenomenon is highly dependent on turbulent flow characteristics. There is indeed a wide range of eddies in the atmospheric boundary layer and they all participate in their own way to the transport and diffusion of the cloud. In particular, the turbulent dispersion of the pollutants is not as effective close to the emission source as opposed to further away: the difficulty of its modelling therefore amounts to correctly taking into account the effect of the different turbulent structures. In this work, the focus is on the atmospheric dispersion modelling at local scale (urban or industrial sites), i.e., for distances of the order of a few kilometres.

The so-called Eulerian models of dispersion are based on the resolution of the advection-diffusion equation on a scalar field corresponding to the concentration of pollutant. This is done by performing a discretisation of this equation in time and space on a mesh. Eulerian models have been used so far at EDF R&D (*Electricité de France*) to model atmospheric dispersion, by means of the computational fluid dynamics (CFD) code *Code_Saturne* and making use of its atmospheric module. On the other hand, the Lagrangian models consist of calculating and tracking the trajectories of particles in a turbulent flow. The cloud of pollutants is discretised and described by a large number of particles emitted into the atmosphere. In this work, the objective is to make use of both the Lagrangian and the atmospheric modules of *Code_Saturne* to model the turbulent dispersion of pollutants with the Lagrangian approach and compare it to the existing results previously obtained with the Eulerian methods.

2 Methodology

Code_Saturne (http://code-saturne.org/) is an open-source CFD code, developed at EDF R&D since 1997. It solves the general equations of fluid mechanics (i.e., continuity equations, momentum, energy and turbulence) using numerical methods and turbulence models. These equations are solved on all types of meshes, including complex unstructured meshes. More details on the numerical methods implemented in the code are provided in Archambeau et al. (2004).

The methodology for stationary dispersion simulations in *Code_Saturne* is the following. Two calculations are performed. The first calculation is used to calculate the dynamical mean fields associated to the wind flow ('*continuous phase*'): velocity, pressure, temperature and turbulence. Once the steady state is reached, this calculation is stopped. The second calculation simulates the dispersion of pollutants within the pre-calculated flow field ('*dispersed phase*'), thus at fixed velocity, pressure and temperature and turbulence fields. The Eulerian and Lagrangian methods used in our work for the dispersion calculation are detailed subsequently. The turbulence models used for our studies are Reynolds-Averaged Navier-Stokes (RANS) models with classical first-order $k - \epsilon$ or second-order $R_{ij} - \epsilon$ closures adapted to the atmosphere and complex geometries.

2.1   Eulerian approach

If we consider a species of concentration c within the pre-calculated flow (assumed to be incompressible), *Code_Saturne* will solve the following advection-diffusion equation:

$$\frac{\partial \langle c \rangle}{\partial t} + \langle U_{f,j} \rangle \frac{\partial \langle c \rangle}{\partial x_j} = \frac{\partial}{\partial x_j} \left(D \frac{\partial \langle c \rangle}{\partial x_j} - \langle U'_{f,j} c' \rangle \right) + \langle S \rangle \ , \tag{1}$$

where $\langle U_{f,j} \rangle$ is the mean velocity of the fluid along the j axis, D the molecular diffusivity and $\langle S \rangle$ the source term.

2.2   Lagrangian approach

Let $\mathbf{X}_p(t)$ be the position of a particle included in the air flow at a time t. Then: $d\mathbf{X}_p = \mathbf{U}_p(t) \ dt$. The movement of each particle included in the flow described by $\mathbf{U}_p(t)$ is governed by Newton's second law. Assuming heavy particles, with a diameter of the same order of magnitude as the Kolmogorov length scale, the equation obtained on the particle velocity is (Minier and Peirano, 2001):

$$\frac{d\mathbf{U}_p}{dt} = \frac{\mathbf{U}_s - \mathbf{U}_p}{\tau_p} + \mathbf{g} \ , \tag{2}$$

where $\mathbf{U}_s$ is the velocity of the fluid sampled through the trajectory of the particle ($\mathbf{U}_s(t) = \mathbf{U}_f(\mathbf{X}_p(t), \ t)$), and τ_p the relaxation timescale of the particle. When τ_p tends to zero, $\mathbf{U}_s$ tends to $\mathbf{U}_p$ and and the limiting case of fluid particles is reached. Thus, every type of particles can be simulated, from gaseous particles to particulate matter.

As the wind flow is calculated using RANS models, we only have access to the statistical mean value of $\mathbf{U}_s$. Thus, in order to close (2), the turbulence effects need to be reconstructed: this is done by introducing a stochastic differential equation modelling the evolution of $\mathbf{U}_s$.

2.3 The SLM (Pope, 1985, 2000)

For the sake of simplicity, let us consider the case of fluid particles, i.e., $\mathbf{U}_s = \mathbf{U}_p$. Then the simplified Langevin model (SLM) is written as follows:

$$dU_{p,i} = -\frac{1}{\rho}\frac{\partial \langle P \rangle}{\partial x_i}\, dt - \frac{U_{p,i} - \langle U_{f,i} \rangle}{T_L}\, dt + \sqrt{C_0 \epsilon}\, dW_i\;, \tag{3}$$

where $\dfrac{\partial \langle P \rangle}{\partial x_i}$ is the mean pressure gradient, C_0 a constant, ϵ the mean dissipation and dW_i a Wiener process of mean 0 and variance dt. Also: $T_L = \dfrac{1}{\frac{1}{2} + \frac{3}{4}C_0}\dfrac{k}{\epsilon}$ is the 'Lagrangian timescale' which actually stands for a particle return-to-isotropy timescale. In the case of the simplified Langevin model, it is isotropic.

It should be noted that the SLM is a particular case of the *generalised Langevin model* also introduced in (Pope, 1985, 2000), which is written as follows:

$$dU_{p,i} = -\frac{1}{\rho}\frac{\partial \langle P \rangle}{\partial x_i} dt + G_{ij}(U_{p,j} - \langle U_{f,j} \rangle)\, dt + \sqrt{C_0 \epsilon}\, dW_i\;. \tag{4}$$

Writing $G_{ij} = -1/T_L\delta_{ij}$, the SLM is retrieved. The SLM has been extensively used especially in turbulent combustion modelling (see Pope, 1985, 1991), in single-phase flow turbulence modelling (Pope, 1994), and also in dispersed turbulent two-phase flows applications (Minier and Peirano, 2001; Minier, 2015). It has also been adapted and used in the context of large-eddy simulation (LES) turbulent dispersion studies, see, for example, Gicquel et al. (2002) or Shotorban and Mashayek (2006).

On the other hand, to our knowledge, this formulation of model with the pressure gradient has not been widely used in the context of atmospheric dispersion. There are several reasons why we have chosen to go further developing it. First, it is written in terms of instantaneous velocity which allows a very simple formulation with the mean pressure-gradient term clearly included in the drift term. It should be highlighted that the presence of this mean-pressure gradient term is what allows the mean-continuity equation to be respected and thus ensures the model to be free of spurious drifts (Pope, 1987; Minier et al., 2014). Historically, in atmospheric studies, to make up for observed spurious drifts in their models, written in terms of fluctuating velocity, several authors heuristically added ad-hoc drift terms (see Lin and Gerbig, 2013). This made the formulation of their models much more complex than if they were written in terms of instantaneous velocity only with the pressure-gradient term. Indeed, the latter formulation requires the calculation of only three gradients, one for each direction, instead of 18 with the formulation written in terms of fluctuating velocity, used by Thomson (1987) for example. Moreover, by construction (see Pope, 2000), the SLM ensures full consistency with the mean Navier-Stokes and the Reynolds equations with Rotta's closure. Finally, no hypothesis is made on the probability density function (PDF) of the velocity of the particles, which was not the case of many of the models used in the atmospheric literature. For instance, Thomson (1987) and derived models assumed the PDF to be Gaussian, but this hypothesis is no longer valid when we move to convective atmospheric boundary layer cases. In these cases, several models following the Thomson (1987) approach and based on non-Gaussian PDFs have been developed: the reader may, for example, refer to Baerentsen and Berkowicz (1984), Luhar et al.

(1996) and Rotach et al. (1996). Another strategy for the convective boundary layer has been proposed in Franzese et al. (1999) and makes no assumption on the form of the PDF of the velocity. Instead, they introduce a simple parameterisation for the drift term in the Langevin equation by approximating it as a quadratic function of velocity. In the case of the SLM, and more generally in the PDF framework developed by Pope, the PDF is a result of the model. It should be noted that no study in highly skewed turbulence conditions has yet been conducted with the SLM, which thus could be the subject of interesting further investigations.

Note that as we have mentioned, in our methodology, we use the formulation of the SLM with instantaneous velocity, that is with the mean-pressure gradient term, because we have access to the fluid mean pressure field through the *Code_Saturne* RANS simulation. In many other models used in the literature, the wind field is computed by a different large hydrostatic scale code, or by a wind field reconstruction code from the measurements. In these cases, the formulation in fluctuating velocity of the SLM, involving the mean quantities $\langle U_{f,i} \rangle$ and $\langle U'_{f,i} U'_{f,j} \rangle$ instead of the mean-pressure gradient term, is recommended. More details on the equivalence between models written in terms of instantaneous and fluctuating velocities can be found in Minier et al. (2014).

3   Well-mixed criterion

The well-mixed criterion states that an initially uniform particle concentration in a turbulent flow should remain uniform. In this section, we will show that the SLM respects this criterion. We studied two cases respectively corresponding to homogeneous and inhomogeneous turbulence. For the case with homogeneous turbulence we found that the criterion was well satisfied (not shown here). In this paper, we present the case of inhomogeneous turbulence which involves an obstacle within a boundary layer. Given the stationary flow corresponding to this situation, we first initialised the domain with uniform particle concentration. Then, we injected, at the inlet, a uniform particle concentration field. We then observed the temporal evolution of the particles (subjected to the mean velocity and turbulence fields relative to the carrier fluid). After a transient time where the particles mix in the domain, a stationary state is reached. The objective is to check if the concentration remains uniform over time.

The mesh is uniform and contains 798,400 cells. The fluid fields and the corresponding boundary conditions are shown on Figure 1. For the fluid phase, we use the second-order $R_{ij} - \epsilon$ Launder, Reece and Rodi (LRR) model with Rotta's closure, which is by construction the model that is fully consistent with the SLM [see Pope (2000) for details].

The time step is $dt = 0.0001 \ s$ – such a value is due to the need to use a time step much smaller than the smallest value of T_L over the fluid domain ($T_{L,min} = 0.001 \ s$). At each time step, 352 particles are injected so that the total number of particles over the domain is about 3,000,000 at convergence, i.e., about four particles per cell, assuming a perfectly uniform repartition. Therefore, it should be noted that starting from a given time step t_0, which should be greater than the time needed for the calculation to reach its steady state, the computed statistics are cumulated over time, in order for them to be reliable. In other words, for any statistical variable Y and for any position $\mathbf{x}$, at each time step $t_n \geq t_0$, the cumulated-over-time statistic $\langle Y \rangle$ is written as follows:

$$\langle Y(\mathbf{x}, t_n) \rangle = \left(Y(\mathbf{x}, t_0) + \sum_{j=1}^{n} \frac{t_j - t_{j-1}}{t_n - t_0} \, Y(\mathbf{x}, t_j) \right) . \tag{5}$$

In our case, we choose to calculate cumulated-over-time statistics after the particles have gone through the whole domain at least once (i.e., the so-called 'advection time' of the particles).

Figure 1 Mean fluid fields, (a) velocity magnitude (m/s) (b) turbulent kinetic energy k (m^2/s^2) (c) turbulent kinetic energy dissipation rate ϵ (m^2/s^3) (see online version for colours)
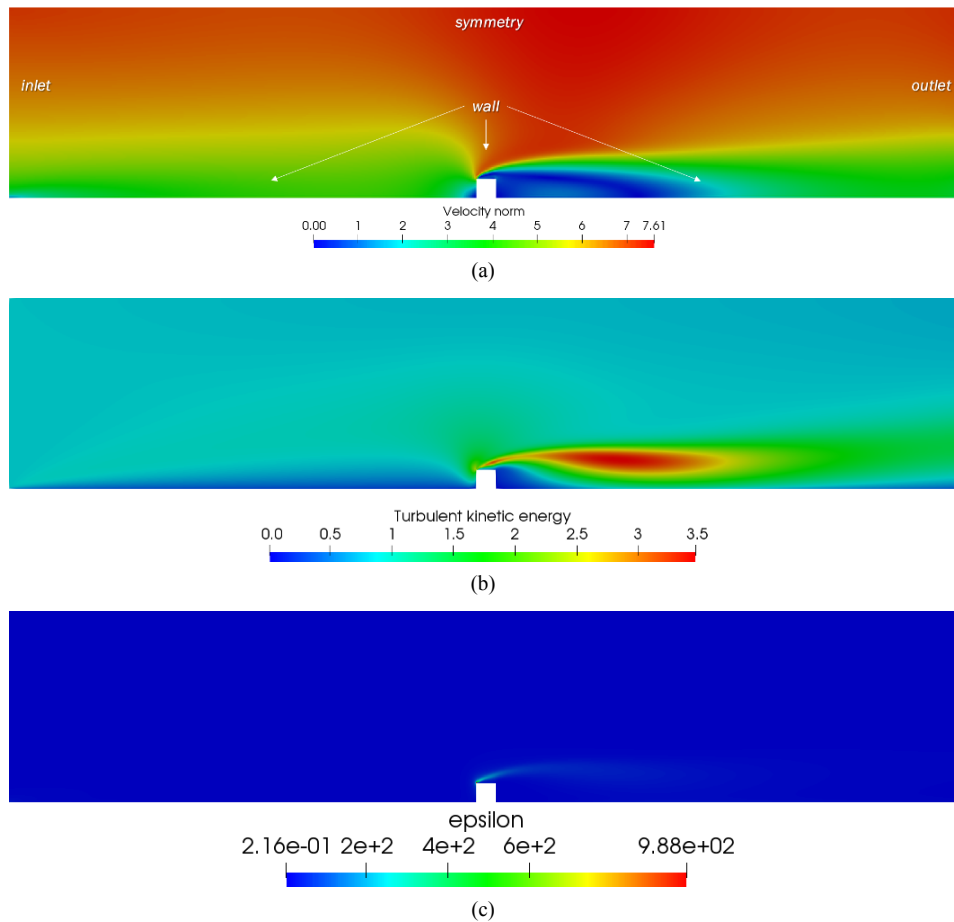
One point is to be made here, answering the following question: what happens if the pressure-gradient term is not properly taken into account in the Langevin equation? Indeed, it has not historically always been the case in the atmospheric Lagrangian models, as we discussed in the previous paragraph. To answer this question, two configurations are examined (see Figure 2, which shows mean normalised concentration fields $c/\langle c \rangle$, where $\langle c \rangle$ is the expected mean concentration given the

particle initialisation). Configuration (a) corresponds to the simulation with a properly taken into account pressure-gradient term and the use of the fully consistent $R_{ij} - \epsilon$ Rotta model, with a close view around the critical zone of the obstacle. Configuration (b) is the same as configuration (a), but removing the pressure-gradient term from the Langevin equation. The configuration (a) shows a uniform concentration (the global spatial error compared to the ideal uniform case is not shown here but is about 5.06% and is mainly due to small discrepancies around the obstacle: locally, in a few cells visible in the close view around the obstacle, the maximum deviation is up to 56%). Obviously the removal of the pressure-gradient term [configuration (b)] leads to important spurious drifts upstream and downstream the obstacle (the global spatial error increases up to 52.8%). This simulation highlights the fact that the pressure-gradient term, as it is such that the mean velocity field satisfies the divergence-free condition, is exactly what makes it possible to maintain a uniform concentration.

Figure 2   Mean normalised concentration field, (a) taking into account pressure-gradient term and use of the fully SLM-consistent $R_{ij} - \epsilon$ Rotta model (b) no pressure-gradient term and use of the fully SLM-consistent $R_{ij} - \epsilon$ Rotta model (see online version for colours)

(a)

(b)
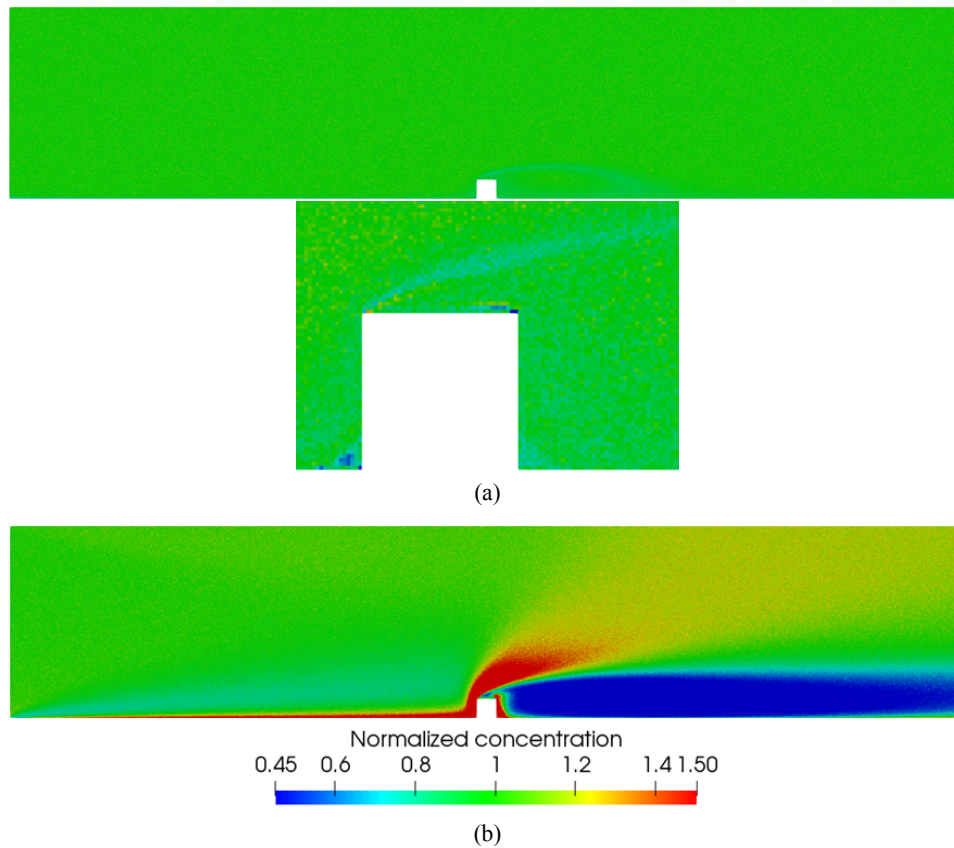
4 Validation case: continuous point release with uniform mean speed and turbulent diffusivity

In this section, the objective is to validate the SLM in the case of a continuous point release (mass flow rate: Q), under uniform mean wind speed and homogeneous turbulence conditions. This study is of interest because under these conditions, there is an analytical solution. It is therefore an opportunity to compare the Lagrangian SLM model with this solution, as well as to observe the differences with the Eulerian model. The solution was first obtained by Taylor with some hypothesis on the form of the autocorrelation function (see Arya, 1999), for the field of maximum concentration as a function of the distance to the source x. It is written as follows:

$$\langle c_{max}(x) \rangle = \frac{Q}{\sqrt{2\pi} \langle U_{f,x} \rangle \sigma_z(x)} \ , \tag{6}$$

where $\sigma_z(x)$ is the plume standard deviation, formulated as follows:

$$\sigma_z(x) = \sigma_{U_{f,x}}(x) \ \frac{x}{\langle U_{f,x} \rangle \sqrt{1 + \dfrac{x}{2\langle U_{f,x} \rangle T_L}}} \ . \tag{7}$$

This formulation, used in numerous atmospheric dispersion codes, allows the well-known discrimination of near-field/far-field regimes of diffusion (see Arya, 1999)). Figure 3 shows the maximum concentration and the normalised plume standard deviation along the axis following the centre of the plume. The objective is to compare both the Eulerian and Lagrangian results to the analytical solution previously introduced. It should be noted that the Eulerian model used here for the calculation of turbulent scalar fluxes is a first-order simple gradient diffusion hypothesis (SGDH) model.

Figure 3 shows that the Lagrangian model provides here much more accurate results than the Eulerian model. This is due to the fact that the Eulerian RANS first-order model (SGDH on the graphs) used in our study is not able to reproduce the different diffusion behaviours between near and far fields. In the near field, there is a rapid spread, while far from the source, the diffusion is slower. This is of course taken into account in the analytical solution through the formulation of the standard deviation [see equation (6) and equation (7)]. By construction – demonstration not shown here, see Pope (2000) for details – this characteristic is also intrinsically included in the Lagrangian model. Figure 3 shows that near the source, there is a sharp and significant drop in concentration for the Lagrangian model and the analytical solution, which means rapid diffusion, whereas the Eulerian model diffuses much more slowly. On the other hand, far from the source, there is a quasi-parallelism between the three curves, which reflects an identical diffusion whatever the approach: the theoretically well-known proportionality of the plume concentration standard deviation to the inverse-distance from the source is retrieved. One important point to be remembered here is that the Eulerian model used for the calculation of turbulent scalar fluxes is an SGDH model, which uses a first-order closure for the advection-diffusion equation. A differential flux model (DFM), or in other words a full second-order RANS model, should yield results more similar to the analytical solution, since it uses a second-order closure that completely transports the turbulent scalar fluxes. However, this model is not completely developed yet and has not been used here.

Figure 3 Maximum concentration and normalised plume standard deviation profiles along the axis following the centre of the plume, (a) maximum concentration along the flow axis (b) normalised plume standard deviation along the flow axis (see online version for colours)

(a)

(b)
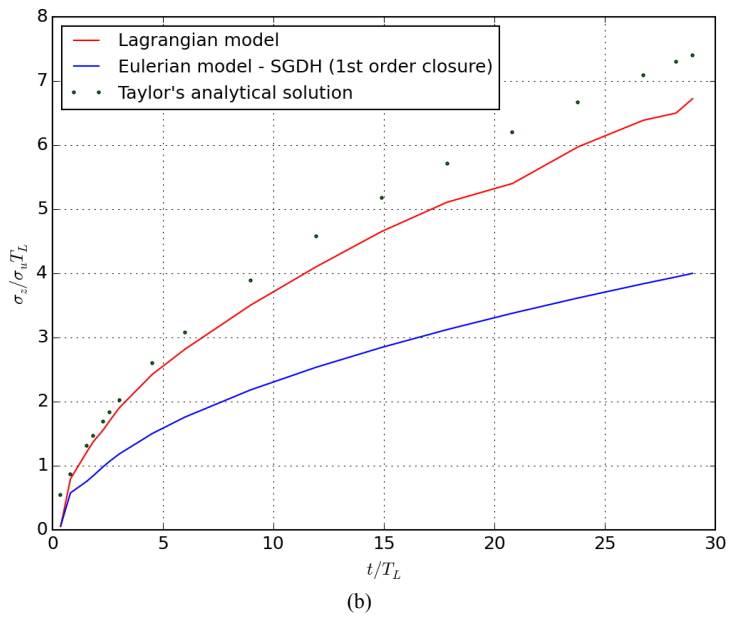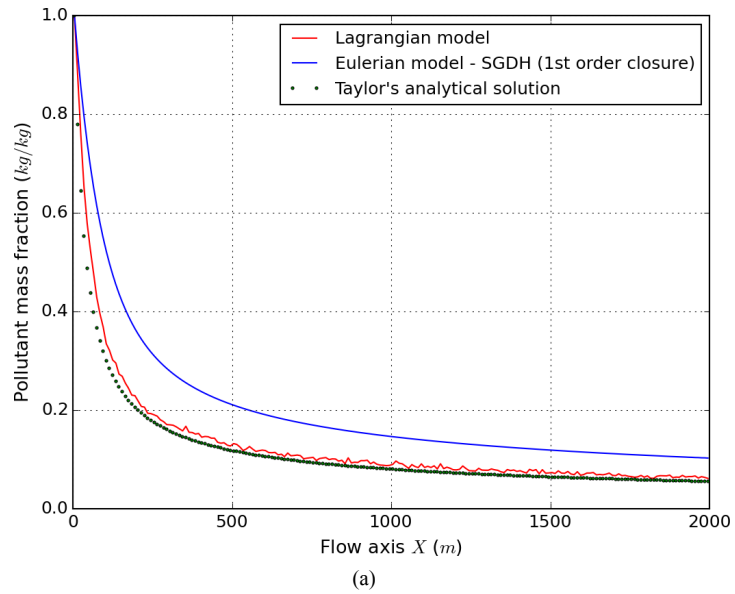
5 Industrial case: SIRTA

The *Site Instrumental de Télédétection Atmosphérique* (SIRTA) site, located in the southern suburb of Paris, is a complex site containing buildings, a lake and area of dense vegetation. In our work, the objective is to simulate in *Code_Saturne* a near-field (50 to 200 m) dispersion experiment carried out on this site in 2015. The experimental campaign involved a stably stratified surface layer and an almost easterly wind. Simulations in *Code_Saturne* of different dispersion experiments at SIRTA have already been performed in the past by Wei et al. (2016) and Chahine et al. (2018). Figure 4 shows a view from the top of the SIRTA site, with a representation of its different zones. The campaign we study is located in zone 1 (in yellow on the figure) and the simulation domain is shown in red on the figure. This area is bounded by a forest to the north and a road to the south. The mesh for the modelling area and the position of the source and the device instruments are also shown in Figure 4.

Figure 4 SIRTA site's map, instrumental devices and mesh (horizontal cross section) for the modelling area (see online version for colours)
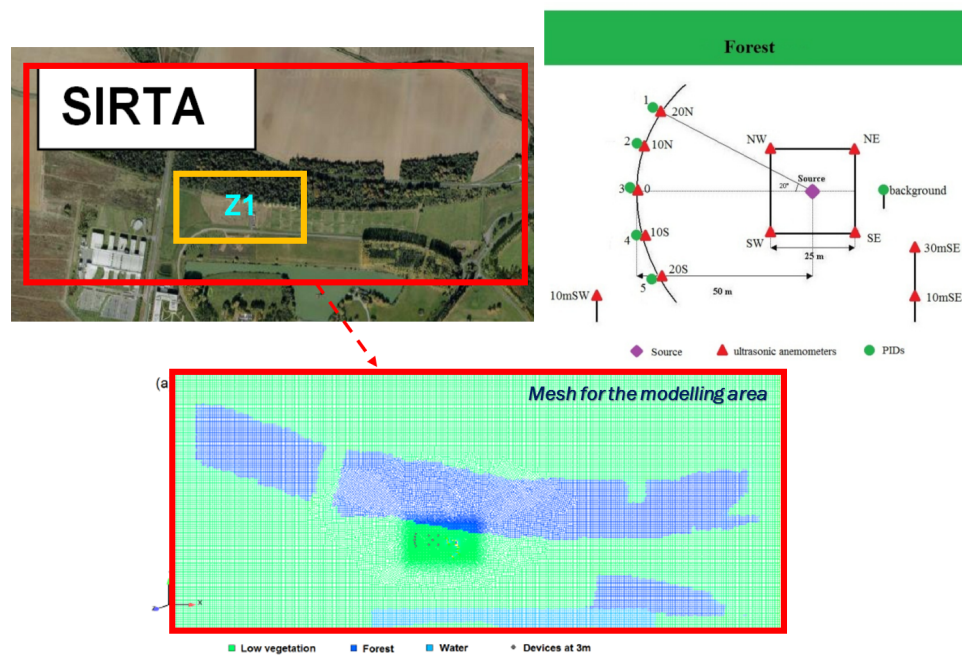
Source: From Wei et al. (2016)

The simulation domain is of dimensions 1,600 m (East-West) × 700 m (North-South) × 200 m (vertical direction). The mesh contains 4,579,071 cells. It is refined near the ground and in the instrumented area. The horizontal resolution ranges from 1 m in the instrumented area (180 m × 100 m) to 5 m for the rest of the computational domain. The vertical resolution ranges from 0.5 m near the ground to 10 m at 200 m height. The buildings upstream the instrumented area are explicitly meshed. As for the ground modelling, a land-use file provided by the *Institut national de l'information*

géographique et forestière (IGN) is used to distinguish the different land cover types (forest, lake) and assign to each of them a corresponding roughness length.

The fluid phase is computed using a RANS $k - \epsilon$ model, with an SGDH closure for the scalars. The boundary conditions are defined as follows:

- Inlet condition of Dirichlet type, with analytical profiles obtained from Monin-Obukhov similarity theory.

- Outlet condition: free outflow.

- Ground, low vegetation and buildings: rough wall, with a roughness length of 0.3 m.

- Lake: rough wall, with a roughness length of 0.0001 m.

As for the forest, it is modelled through an analogy with a porous media. We modify the $k - \epsilon$ model equations in order to simulate the momentum losses and turbulence generation within the forest. Indeed, the canopy creates a drag force opposed to the flow, which reduces the wind velocity and modifies the turbulence fields. This model has been developed and used by Sanz (2003), Katul et al. (2004), Dalpé and Masson (2009), Zaïdi et al. (2013) and Wei et al. (2016). For earlier relevant references for the study of canopy flow, the reader may refer to Wilson and Shaw (1977), or Shaw and Schumann (1992) who used LES simulations. The added source term in the Navier-Stokes momentum equation is written as follows:

$$S_{u,i} = -\rho \alpha C_d |\mathbf{U}_f| U_{f,i} \tag{8}$$

where ρ is the air density, α the leaf area density and C_d the drag coefficient of the forest. In our study, $C_d = 0.2$ and $\alpha = 0.5$ m^{-1}. The turbulence source terms S_k and S_ϵ in the k and ϵ equations are expressed as:

$$S_k = \rho \alpha C_d \beta_p |\mathbf{U}_f|^3 - \rho \alpha C_d \beta_d k |\mathbf{U}_f| \ , \tag{9}$$

$$S_\epsilon = \rho \alpha C_d C_{\epsilon 4} \beta_p \frac{\epsilon}{k} |\mathbf{U}_f|^3 - \rho \alpha C_d C_{\epsilon 5} \beta_d \epsilon |\mathbf{U}_f| \ , \tag{10}$$

where β_p, β_d, $C_{\epsilon 4}$ and $C_{\epsilon 5}$ are constants of the model, expressed as follows:

$$\beta_p = 1 \ , \tag{11a}$$

$$\beta_d = \sqrt{C_\mu} \left(\frac{2}{0.05} \right)^{2/3} \beta_p + \frac{3}{\sigma_k} = 5.03 \ , \tag{11b}$$

$$C_{\epsilon 4} = C_{\epsilon 5} = \sigma_k \left[\left(\left(\frac{2}{\sigma_\epsilon} - \sqrt{C_\mu} \right) / 6 \right) \left(\frac{2}{0.05} \right)^{2/3} (C_{\epsilon 2} - C_{\epsilon 1}) \right] = 0.9 \ , \tag{11c}$$

where the set of constants (C_μ, $C_{\epsilon 1}$, $C_{\epsilon 2}$, σ_k, σ_ϵ) takes the following values given by Launder and Spalding's (1974) standard model:

C_μ	$C_{\epsilon 1}$	$C_{\epsilon 2}$	σ_k	σ_ϵ
0.09	1.44	1.92	1.0	1.3

Within this flow field, the pollutant (propylene, C_3H_6) is continuously injected through a scalar source term, with the imposed pollutant mass flow of 200 L/min. As for the Lagrangian approach, 20,000 particles per time step are injected, with the same imposed mass flow.

Figures 5 and 6 show the results through the comparison of the mean concentrations (*ppmv*) between measurements and simulations for the six points of measurements described in Figure 4 (green points corresponding to the 'PID' – photoIonisation detectors – caption). PID 1 to 5 are located at $z = 3$ m and PID 6 is not shown on Figure 4 but is located at $z = 10$ m over PID 3.

Generally speaking, the results given by the Lagrangian and Eulerian models are close, though we can observe in Figure 6 greater vertical diffusion with the Lagrangian SLM than with the Eulerian model, hence the lower concentrations at $z = 3$ m observed in Figure 5. The important vertical diffusion observed with the SLM is believed to be due to the fact that the SLM is a simple model with a linear return-to-isotropy assumption. The G_{ij} tensor of equation (4) is diagonal and isotropic ($G_{ii} = -1/T_L$). A more advanced model, such as for instance the Launder, Reece, Rodi – isotropisation of production (LRR-IP) model, adds to the Rotta model a contribution called 'isotropisation of production', which increases the Reynolds-stress anisotropy (see Pope, 2000). This model could therefore be an interesting path for further investigations.

Figure 5 Comparison of the mean concentrations (*ppmv*) between measurements and simulations – PID 1 to 5 (see online version for colours)
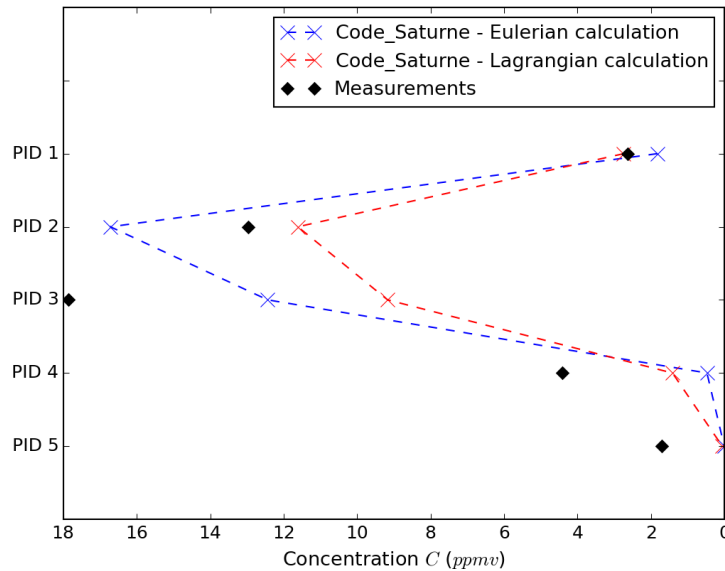
Notes: The plume corresponds to the sketch of the instrumented zone and the source shown in Figure 4, for a more visual representation.

Figure 6 Comparison of the mean concentrations (*ppmv*) between measurements and simulations – vertical profile – PID 3 and 6 (see online version for colours)
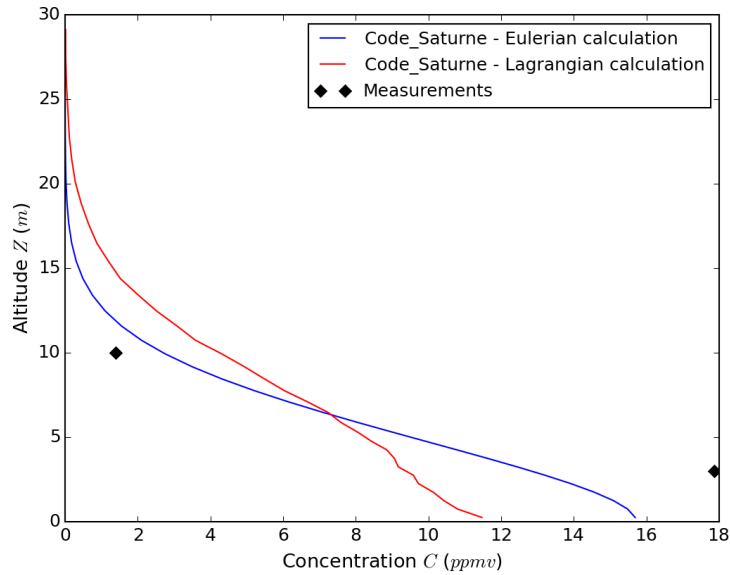
Figure 7 Normalised concentration along the axis following the centre of the plume (see online version for colours)
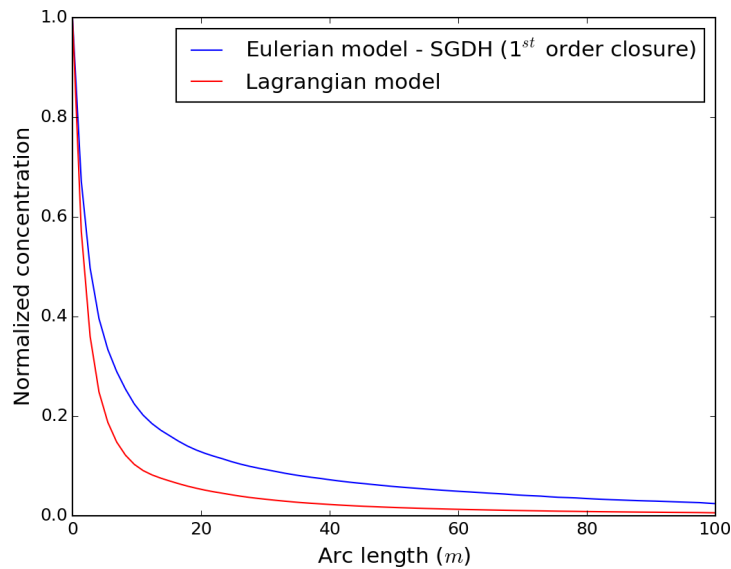
An interesting point is that the zone we are interested in, at a distance of 50 m, is already considered as 'far field', where both models are expected to show the same diffusion behaviour. Indeed, when speaking about near and far fields, one has to remember that it is always in comparison to the value of T_L. At the injection cell, the fluid velocity is

about 1.4 m/s and T_L = 8.8 s. Therefore, the near-field region corresponds to distances approximately below $1.4 \times 8.8 \approx 12$ m. As the PID are located at a distance of 50 m, they are already located in the 'far-field region'. Figure 7 shows the concentration along the axis following the centre of the plume, computed by both the Eulerian and Lagrangian approaches. This concentration is normalised by its maximum value obtained at the injection cell. Exactly as for the analytical case presented in the previous section, we can observe the ability of the Lagrangian model to reproduce the difference of behaviours between near and far fields. In the near field, that is to say for distances below approximately 12 metres, the Lagrangian model shows a rapid spread, which slows down for higher distances. We can also observe the logical tendency of both the Lagrangian and Eulerian curves to become parallel starting from this distance. Once again, one has to remember that these results are due to the fact that the Eulerian and Lagrangian models used here are not at the same level of closure. The Eulerian model uses a first-order turbulence closure whereas the Lagrangian model (SLM) is second-order. A full second-order Eulerian model would be expected to provide similar results as the Lagrangian model and is in fact the subject of further investigations.

Finally, to sum up, one important conclusion from this analysis is that as long as the source is located in a small-T_L region, then the 'near-field' region will stay close to the source. This will actually happen for all near-ground releases in general, as also mentioned in Näslund et al. (1994), given that T_L takes small values near the ground. In these cases, the usefulness of a Lagrangian Langevin model is therefore restricted and an Eulerian first-order model would be a satisfactory option.

6 Conclusions

The objective of this work is to develop a Lagrangian stochastic tool to simulate atmospheric dispersion simultaneously with Eulerian dispersion, within the CFD code *Code_Saturne*. After choosing to work with the SLM (Pope, 1985, 2000), we have validated this model for several situations. First we have ensured that our model respects the well-mixed criterion, considering a general case of inhomogeneous turbulence. In the latter case, we have shown that the pressure-gradient term is exactly what allows the well-mixed criterion to be fulfilled. Then, we have also validated the SLM by checking with an analytical solution and have shown indeed the well-known distinction by the model of the two regimes of diffusion (near and far fields). Finally, to this date, we are currently validating the model for several industrial cases. Results have been shown in this paper for the SIRTA campaign, using a RANS $k - \epsilon$ model for the fluid phase. Further investigations are to be conducted on the use of the $R_{ij} - \epsilon$ model, as this requires the development of the right turbulence source terms corresponding to this model.

Acknowledgements

References

Archambeau, F., Méchitoua, N. and Sakiz, M. (2004) 'Code saturne: a finite volume code for the computation of turbulent incompressible flows – industrial applications', *International Journal on Finite Volumes*, Vol. 1, pp.1–62.

Arya, S.P. (1999) *Air Pollution Meteorology and Dispersion*, Oxford University Press, Oxford.

Baerentsen, J.H. and Berkowicz, R. (1984) 'Monte Carlo simulation of plume dispersion in the convective boundary layer', *Atmospheric Environment*, Vol. 18, No. 4, pp.701–712.

Chahine, A., Dupont, E., Musson-Genon, L., Legorgeu, C. and Carissimo, B. (2018) 'Long-term modeling of the dynamical atmospheric flows over SIRTA site', *Journal of Wind Engineering and Industrial Aerodynamics*, Vol. 172, pp.351–366.

Dalpé, B. and Masson, C. (2009) 'Numerical simulation of wind flow near a forest edge', *Journal of Wind Engineering and Industrial Aerodynamics*, Vol. 97, No. 5, pp.351–366.

Franzese, P., Luhar, A.K. and Borgas, M.S. (1999) 'An efficient Lagrangian stochastic model of vertical dispersion in the convective boundary layer', *Atmospheric Environment*, Vol. 33, No. 15, pp.2337–2345.

Gicquel, L.Y., Givi, P., Jaberi, F.A. and Pope, S.B. (2002) 'Velocity filtered density function for large eddy simulation of turbulent flows', *Physics of Fluids*, Vol. 14, No. 3, pp.1196–1213.

Katul, G.G., Mahrt, L., Poggi, D. and Sanz, C. (2004) 'One- and two-equation models for canopy turbulence', *Boundary-Layer Meteorology*, Vol. 113, No. 1, pp.81–109.

Launder, B.E. and Spalding, D.B. (1974) 'The numerical computation of turbulent flows', *Computer Methods in Applied Mechanics and Engineering*, Vol. 3, No. 2, pp.269–289.

Lin, J.C. and Gerbig, C. (2013) 'How can we satisfy the well-mixed criterion in highly inhomogeneous flows? A practical approach', *Lagrangian Modeling of the Atmosphere*, Vol. 200, pp.59–69.

Luhar, A.K., Hibberd, M.F. and Hurley, P.J. (1996) 'Comparison of closure schemes used to specify the velocity PDF in Lagrangian stochastic dispersion models for convective conditions', *Atmospheric Environment*, Vol. 30, No. 9, pp.1407–1418.

Minier, J-P. (2015) 'On Lagrangian stochastic methods for turbulent polydisperse two-phase reactive flows', *Progress in Energy and Combustion Science*, Vol. 50, pp.1–62.

Minier, J-P., Chibbaro, S. and Pope, S.B. (2014) 'Guidelines for the formulation of Lagrangian stochastic models for particle simulations of single-phase and dispersed two-phase turbulent flows', *Physics of Fluids*, Vol. 26, No. 11, pp.113–303.

Minier, J-P. and Peirano, E. (2001) 'The PDF approach to turbulent polydispersed two-phase flows', *Physics Reports*, Vol. 352, No. 1, pp.1–214.

Näslund, E., Rodean, H.C. and Nasstrom, J.S. (1994) 'A comparison between two stochastic diffusion models in a complex three-dimensional flow', *Boundary-Layer Meteorology*, Vol. 67, No. 4, pp.369–384.

Pope, S.B. (1985) 'PDF methods for turbulent reactive flows', *Progress in Energy and Combustion Science*, Vol. 352, No. 1, pp.119–192.

Pope, S.B. (1987) 'Consistency conditions for random-walk models of turbulent dispersion', *Physics of Fluids*, Vol. 30, No. 8, pp.2374–2379.

Pope, S.B. (1991) 'Computations of turbulent combustion: progress and challenges', *Symposium (International) on Combustion*, Vol. 23, pp.591–612.

Pope, S.B. (1994) 'Lagrangian PDF methods for turbulent flows', *Annual review of Fluid Mechanics*, Vol. 26, No. 1, pp.23–63.

Pope, S.B. (2000) *Turbulent Flows*, Cambridge University Press, Cambridge.

Rotach, M.W., Gryning, S.E. and Tassone, C. (1996) 'A two-dimensional Lagrangian stochastic dispersion model for daytime conditions', *Quarterly Journal of the Royal Meteorological Society*, Vol. 122, No. 530, pp.367–389.

Sanz, C. (2003) 'A note on k-ε modelling of vegetation canopy air-flows', *Boundary-Layer Meteorology*, Vol. 108, No. 1, pp.191–197.

Shaw, R.H. and Schumann, U. (1992) 'Large-eddy simulation of turbulent flow above and within a forest', *Boundary-Layer Meteorology*, Vol. 61, Nos. 1–2, pp.47–64.

Shotorban, B. and Mashayek, F. (2006) 'A stochastic model for particle motion in large-eddy simulation', *Journal of Turbulence*, Vol. 7, N18.

Thomson, D.J. (1987) 'Criteria for the selection of stochastic models of particle trajectories in turbulent flows', *Journal of Fluid Mechanics*, Vol. 180, pp.529–556.

Wei, X., Dupont, E., Carissimo, B., Gilbert, E. and Musson-Genon, L. (2016) 'Near-field pollutants dispersion in a stratified surface layer: comparison of numerical study and field measurements of SIRTA', *Air Pollution Modeling and its Application*, Vol. 24, pp.365–389.

Wilson, N.R. and Shaw, R.H. (1977) 'A higher order closure model for canopy flow', *Journal of Applied Meteorology*, Vol. 16, No. 11, pp.1197–1205.

Zaïdi, H., Dupont, E., Milliez, M., Musson-Genon, L. and Carissimo, B. (2013) 'Numerical simulations of the microscale heterogeneities of turbulence observed on a complex site', *Boundary-Layer Meteorology*, Vol. 147, No. 2, pp.237–259.